

# Therapeutic potential of Bama miniature pig adipose stem cells induced hepatocytes in a mouse model with acute liver failure

Shuang Zhang · Zhiqiang Zhu · Yufeng Wang · Shi Liu · Chenqiong Zhao · Weijun Guan · Yuhua Zhao

Received: 9 October 2017 / Accepted: 1 February 2018 / Published online: 7 March 2018  
© Springer Science+Business Media B.V., part of Springer Nature 2018

**Abstract** The role of mesenchymal stem cells (MSCs) in cellular therapy is well recognized in this work. MSCs have advantages of high proliferation, clone formation, multi-lineage differentiation and immunosuppression. Furthermore, adipose-resident MSCs (ADSCs) are extensively employed due to its advantages of abundant source, low cost and simple operation. Many researchers have emphasized the role of adipose-resident MSCs in the development of therapies for liver injury, but few attentions were paid on the use of induced functional hepatocytes. Therefore, in this work the role of adipose-resident MSCs induced functional hepatocytes was mainly investigated. The function of induced hepatocytes by ELISA and the induction rate was confirmed by flow cytometry and evaluated by experimental observations. The induced hepatocytes were firstly transplanted into CCl<sub>4</sub>-caused liver damage ICR mice by tail vein. After transplantation, both liver fibrosis and function could be improved by hepatocytes, which were examined

through histology, immunofluorescence staining, serum profile and biochemical parameters levels. The production of cytokines was then compared with normal mice and injury mice to explore the therapeutic mechanisms of hepatocytes. Finally, the secretions of TGF- $\beta$ 1, IL-6 and IL-10 in hepatocytes transplanted mice were determined and found to be higher than that of the normal and injury mice. The hepatocytes derived from ADSCs were proven to have a great significance in the therapeutic efficacy and clinical settings of liver disease animal models.

**Keywords** Adipose tissue · Hepatocytes · Liver injury · Cell therapy

## Introduction

Liver disease can be caused by hereditary syndromes, metabolic and autoimmune diseases, infected and vascular conditions, which could weaken the function of liver (Schueller et al. 2017). Liver damage is mainly divided into two categories: acute and chronic disease. Chronic liver damage is a long-term process and can develop into liver fibrosis, cirrhosis and hepatocellular carcinoma (Asrani et al. 2013). It is a hard issue to treat this kind of disease. Except liver transplantation, there is no other effective therapy to such disease at the terminal stage (Terai et al. 2006). Acute liver failure (ALF) can be further improved by liver

---

S. Zhang · Z. Zhu · Y. Wang · S. Liu · C. Zhao · Y. Zhao (✉)  
Research Center for Sports Scientific Experiment, Harbin Sport University, Harbin, China  
e-mail: zhaoyuhua2017@outlook.com

W. Guan  
Department of Animal Genetic Resources, Institute of Animal Science, Chinese Academy of Agricultural Sciences, Beijing, China  
e-mail: weijunguan301@gmail.com

transplantation, but still holding a 55–75% rate of mortality (Mendizabal and Silva 2016). However, the transplantation of liver is limited by high costs, shortage of donor organs and an invasive procedure (Dhawan et al. 2010). Therefore, liver cells transplantation has become a viable substitute to liver transplantation in some liver diseases, but it is restricted by organ donors and the low cell quality of available liver tissues (Zaret and Grompe 2008; Terry et al. 2007).

Adipose tissue has many advantages, such as abundant source, low cost, simple operation and safety. It can be obtained through invasive liposuction. Adipose-derived mesenchymal stem cells (ADSCs) are rather abundant and can be easily isolated and cultured. Meanwhile, ADSCs have a lower immunogenicity and are multipotent, which all provide the basis for the application of ADSCs in tissue engineering (Zhang et al. 2017a, b).

Furthermore, ADSCs could be induced into hepatocytes both *in vitro* (Ong et al. 2006a, b; Lee et al. 2004) and *in vivo* (Zhan et al. 2006), which remains to be controversial whether the liver can be completely regenerated *in vivo* through ADSCs transplantation or not. The potential of ADSCs to differentiate into hepatocytes and immunomodulatory properties (Volarevic et al. 2011) constructed the way for ADSCs in the treatment of hepatic fibrosis. Therefore, the ability of ADSCs induced-hepatocytes to reduce fibrosis degree and recover hepatic function in a severe acute liver damage mouse model was comprehensively explored.

## Materials and methods

### Animals

Bama miniature Pig (1 day postnatal from 8 individuals, 4 males and 8 females) were supplied by the Chinese Academy of Agriculture Sciences, (Beijing, China). Six-week-old ICR male mice weighing 20 g were used in this investigation. Mice were obtained from BEIJING HFK Bio-science (Beijing, China, <http://www.labagd.com>). Animals were performed in accordance with the criteria outlined in the “Guide for the Care and Use of Laboratory Animals” prepared by the National Academy of Sciences and published by the National Institutes of Health (NIH publication 86-23 revised 1985). All animal experiments were performed according to international

guidelines and approved by the ethics committee of the Chinese Academy of Agricultural Sciences, Beijing, China (Permit Number: IAS10012).

### Isolation, culture, and purification of ADSCs

The protocols used for isolation and cultivation of 1 day postnatal bama miniature pig adipose tissue derived stem cells are following the previous procedures (Zhang et al. 2017a, b). The bama miniature pigs were euthanized after deep anaesthesia. Adipose tissues was harvested from visceral (omental region) of miniature pigs under aseptic condition and washed with phosphate-buffered saline (PBS). The extracellular matrix was dissociated with 0.1% (m/v) type-I collagenase (Sigma, St. Louis, MO, USA) for 1 h at 37 °C after removing the blood vessels and fascia. The suspension was filtered through a 74- $\mu$ m mesh sieve and centrifuged at 1200 rpm for 8 min. Cells were cultured in complete medium (L-DMEM) (Gibco, NY, USA), 10% (v/v) FBS (Biocrom, Berlin, Germany), 10 ng/mL basic fibroblast growth factor (Peprotech, Rocky Hill, NJ, USA), 2 mM L-glutamine, 1% B-27 (m/v) (Gibco), and  $10^4$  IU/mL penicillin/streptomycin (Gibco, NY, USA) (Zhang et al. 2017a, b). Cells were digested with 0.125% (w/v) trypsin–EDTA when they reached 70–80% confluence and were homogeneous after 3–4 passages.

### Immunofluorescence

Cells were incubated for 1 h in the following antibodies: (1) mouse anti-pig CD29 (1:100; Abcam); (2) rat anti-pig CD44 (1:100; Abcam, Cambridge, MA, USA); and (3) mouse anti-pig CD90 (1:100; Abcam); (4) mouse anti-pig CD105 (1:100; Abcam) and finally observed by Nikon TE-2000-E confocal microscope (Nikon, SHanghai, China) (Bai et al. 2013).

### RNA isolation and RT-PCR

RNA was extracted from passage-4 cells, passage-14 cells, passage-20 cells and passage-26 cells using Trizol reagent (Invitrogen, Carlsbad, CA, USA). The TaKaRa RNA PCR Kit (AMV) Ver.3.0 was employed for reverse transcription polymerase chain reaction. The cDNA was amplified by Emerald Amp Max PCR (TaKaRa, Dalian, China). Products were confirmed by gel electrophoresis (Ma et al. 2017).

### Osteogenic differentiation and confirmation

ADSCs at passage-18 were plated on 60-mm dishes for osteogenic differentiation. The cells were incubated with osteogenic induction medium (L-DMEM, 10% FBS (v/v), 100 nM dexamethasone (Sigma, USA), 250 mM L-ascorbic acid-2 phosphate (Sigma, USA) and 10 mM  $\beta$ -glycerophosphate (Sigma, USA)) when they reached 80% confluence. The control group was fed with DMEM medium. At 10 and 22 days after induction, cells were fixed by 4% paraformaldehyde (m/v) and stained with alizarin (Beijing, China) to visualize the mineralised matrix. The osteogenic specific genes OPN, RUNX2 were detected by RT-PCR.

### Epithelial cells differentiation and confirmation

ADSCs of passage-8 were incubated on 6-well plates. At confluence of 50%, we changed the medium into L-DMEM medium containing 10% FBS(v/v), 1% B27 (Gibco, USA), 1% glutamine (Gibco, USA), 1% streptomycin (Gibco, USA), 10 ng/mL bFGF (Pepro- tech, Rocky Hill, NJ, USA) and 15 ng/mL EGF (Pepro- tech, Rocky Hill, NJ, USA). After 10 days, the cells were analyzed by immunofluorescent assays for the epithelial marker gene CK19. The epithelial specific genes CK19 and E-caderin were detected by RT-PCR.

### Functional hepatic differentiation and confirmation

Passage-13 ADSCs were incubated on 60-mm plates. When the cells reached confluence of 50%, the medium was renewed with hepatic inducing medium (L-DMEM, 5% FBS (v/v), 20 ng/mL FGF-4 (Pepro- tech, Rocky Hill, NJ, USA), 20 ng/mL HGF (Pepro- tech, Rocky Hill, NJ, USA), 40 nmol/mL dexamethasone (Sigma, USA) and 1% ITS (Pepro- tech, Rocky Hill, NJ, USA)). 15 days later, the cells were detected by PAS staining. Cells were fixed with paraformaldehyde for 20 mins and oxidized in periodic acid Schiff (PAS) (Sigma, USA) for 5 mins to visualize the glycogen deposits. Then cells were incubated with Schiff's reagent for 15mins and counterstained with hematoxylin for 2 mins. The hepatic specific genes AFP, ALB were detected by RT-PCR.

### Immunofluorescence staining

Cells were incubated with ALB antibody (1:200, Abcam, USA) at 4 °C overnight. Then they were incubated with secondary antibodies (1:200) (Bioss, China) at room temperature. Finally, counter-staining with DAPI at room temperature was employed and results were examined by Nikon-TE-2000.

### Efficiency of differentiation

Efficiency of differentiation was evaluated by fluorescence-activated cell sorting (FACS) by Albumin (ALB).  $1 \times 10^6$  Induced hepatocytes were harvested and fixed with 4% PFA for 30 mins at room temperature, and then permeabilized in staining buffer for 10 mins. Cells were then incubated with primary antibody: ALB (Abcam, USA) for 60 mins. The cells were washed with PBS and stained by FITC-labeled goat anti-sheep immunoglobulin (Bioss, China). Cells were analyzed by the FC500 flow cytometry (Backman) and the data was evaluated by EPICS-XL flow cytometry.

### Albumin and urea secretion by enzyme-linked immunosorbent assay (ELISA)

The supernatant from hepatic induction medium was harvested on the 14th day. According to the manual guideline, the albumin and urea concentration were determined by ELISA Quantitation Kit (Exocell Inc., Philadelphia, PA, USA).

### Chronic liver fibrosis model in mice and liver damage model evaluation

Mice were given one injection of either 200  $\mu$ L of mineral oil (control) or 10% solution of  $\text{CCl}_4$  in mineral oil via an intraperitoneal route twice a week (Khurana and Mukhopadhyay 2007). After 4 weeks injury, some mice were submitted to serological tests and histologic analyses for the evaluation of the animal model. Mice were separated into three groups, 18 mice of each group were randomly designated as a cell transplantation group, control group and normal group, as shown in Table 1.

**Table 1** Summary of animal groups

	No. of animals	Transplanted cells	Application site	Week of sacrifice
Injury	6	Hepatocytes	Caudal vein	5
	6	Hepatocytes	Caudal vein	6
	6	Hepatocytes	Caudal vein	7
Control	6	PBS	Caudal vein	5
	6	PBS	Caudal vein	6
	6	PBS	Caudal vein	7
Normal	6			5
	6			6
	6			7

### Cell labeling with CM-Dil

In order to analyze bio-distribution after injection into the vein,  $1.5 \times 10^7$  hepatocytes were labeled with CM-Dil before injection (Carvalho et al. 2008). Cell suspension was dissolved in dimethylsulfoxide (DMSO) 2 mg/mL (0.2% w/v). 150  $\mu$ L of stock solution was added to the cell suspension in 15 mL medium and the mixture was incubated at 37 °C for 5 min. Then, the mixtures were transferred to 4 °C for another 15 min. After centrifugation (2000 rpm for 8 min), only cells were collected and washed again in saline solution. The pellet was re-suspended in PBS and injected into mice through the caudal vein. Six animals in each group were analyzed on the 1st, 2nd, and 3rd week after cell transplantation. Injected cells were evaluated by frozen slice.

### Transplantation of hepatocytes into ICR injured mice

For cell transplantation,  $1.5 \times 10^7$  hepatocytes (P8) suspended in 50  $\mu$ L phosphate buffered saline (PBS) were subjected to vein grafts into mice injected with CCl<sub>4</sub> for 3 weeks (n = 18) (Table 1). For control group, 50  $\mu$ L PBS was intravenously injected into mice after 3 weeks of CCl<sub>4</sub> treatment (n = 18). After transplantation, additional 1, 2 and 3-week treatments of CCl<sub>4</sub> twice a week were performed to the mice. Livers and peripheral blood were harvested at different intervals.

### Serum and liver tissue analysis

In order to evaluate the enzyme level of liver injury, serum ALT, AST, ALB, TP, GLOB, TGF- $\beta$ , IL-6 and

IL-10 levels were measured by Activity Assay Kits (Sigma, USA) according to the manipulation. Furthermore, the evaluation for the liver injury was carried out through histological staining. Five-micrometer liver tissue was cut down and stained with hematoxylin and eosin (H&E) and masson according to standard protocols (Wei et al. 2014).

### Immunohistochemistry

To detect the distribution and survival of hepatocytes, the pig specific anti-serum CK18 (1: 1000; Abcam) was added to blocking medium. The cell distributions at 1, 2 and 3-week intervals after transplantation were examined and analyzed by a con-focal optical system (Nikon, TE2000).

### Statistical analysis

Data were examined by ANOVA. Differences between three sets were assessed by a Tukey–Kramer test. 0.05 was configured as the threshold of *P* value for significance.

## Results

### Characterization of MSCs derived from pig adipose (ADSCs)

ADSCs grew in a spindle like morphology when cultured for 3 days, and they were cultured up to passage-27 eventually (Fig. 1a). Results presented that ADSCs expressed primitive cell markers (CD29, CD44, CD90 and CD105) on day 3 (Fig. 1b). Cells at passage-4, passage-14, passage-20 and passage-25



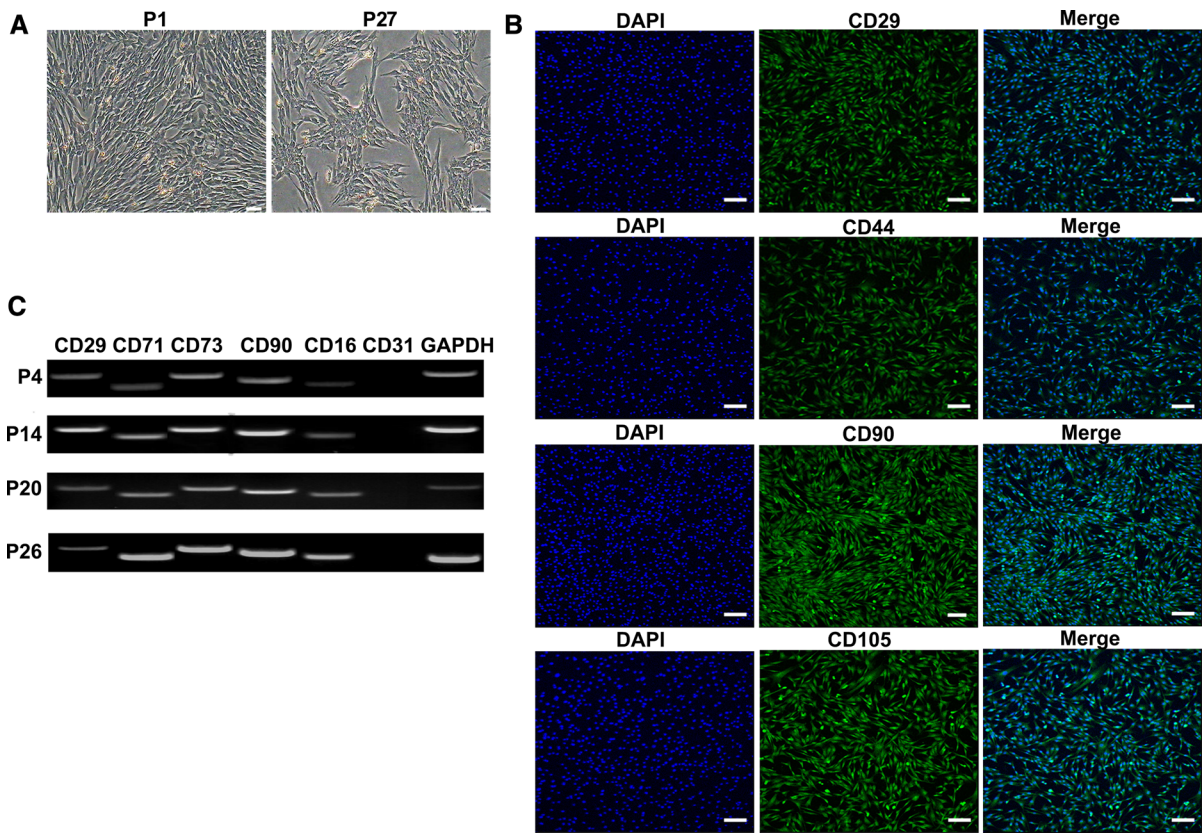


**Fig. 1** Analysis of ADSCs. **a** Morphology of ADSCs. (bar = 100 μm). **b** Immunofluorescence staining revealed that the cells were positive for CD29, CD44, CD90 and CD105 were (scale bar = 50 μm). **c** RT-PCR results presented that ADSCs

at passage 4, passage 14, passage 20 and passage 26 expressed CD29, CD71, CD73, CD90 and CD166, but did not express CD31. GAPDH was used as control

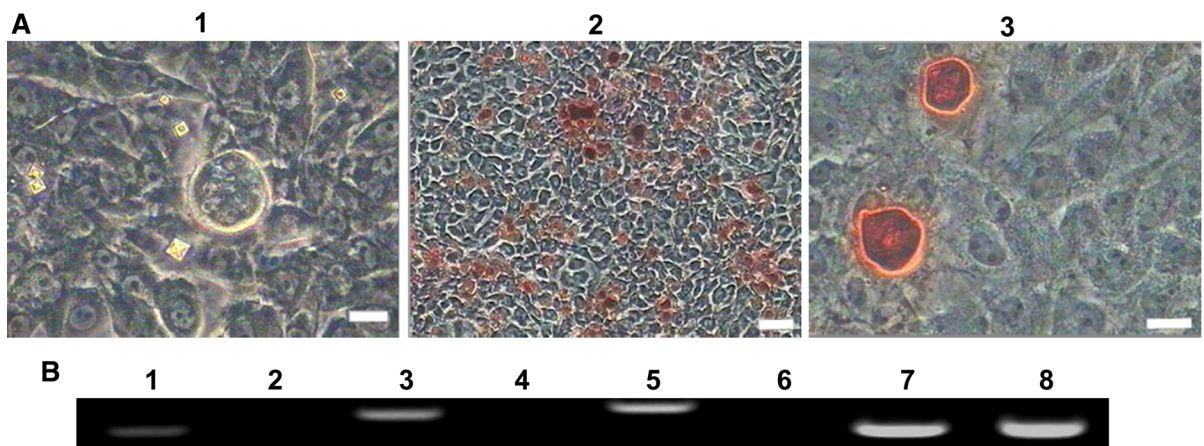


**Fig. 2** Osteogenic induction of ADSCs. **a** Morphology of osteoblasts. (1) Pre-stain, (2 and 3) staining at ×40 and ×200 (bar = 100 μm). **b** RT-PCR detection of osteogenic specific genes OPN, RUNX2 and COL1A2. 1, 3 and 5 for the induced

group, 2, 4 and 6 for the control group, 7 and 8 for GAPDH. Lane 1 and 2 are OPN, lane 3 and 4 are RUNX2, lane 5 and 6 are COL1A2

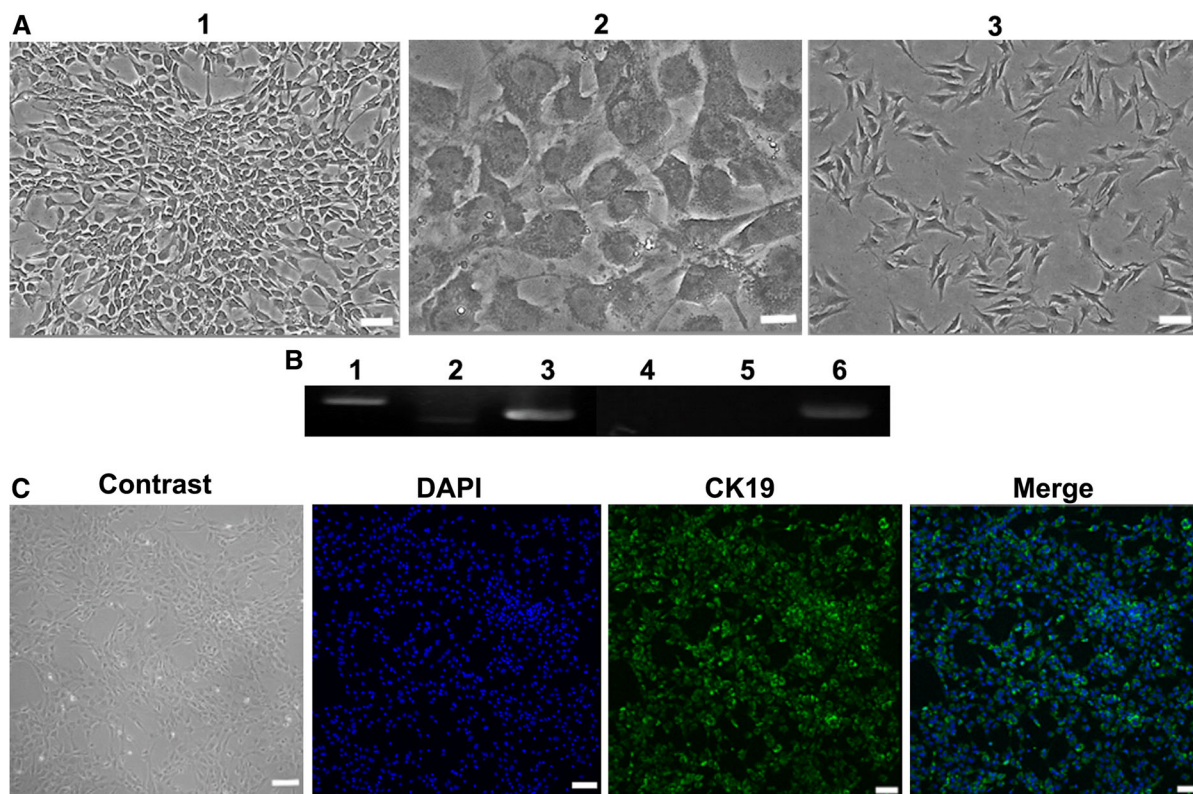


**Fig. 3** Epithelial cells induction of ADSCs. **a** Morphology of epithelial cells. (1 and 2) After 10 days induction, epithelioid cells presented a pebble like morphology. Cells showed indistinct boundaries, obvious refraction, and stereoscopic morphology. (3) There was no obvious change in the control group. Scale bar = 100  $\mu$ m. **b** RT-PCR analysis of specific

genes (E-cadherin and CK19). 1, 2 and 3 for the induced group; 4, 5 and 6 for the control group; 1 and 4 were E-cadherin, 2 and 5 were CK19, 3 and 6 were GAPDH. **c** Immunofluorescence analysis: induced group cells were positive for the specific anti CK19 antibody. Scale bar = 100  $\mu$ m

were analyzed by RT-PCR and they all expressed CD29, CD71, CD73, CD90, CD166 but did not express CD31 (Fig. 1c). The potential ability of ADSCs was explored and calcium deposits were found in the osteogenic differentiation. Results were assessed by alizarin stain and RT-PCR. The induced epithelial-like cells presented cobblestone appearance and were positive for the specific antibody CK19. Results were tested by alizarin staining, RT-PCR and immunofluorescence (Figs. 2 and 3). In conclusion, ADSCs had a feature of multipotency.

#### Function of hepatic-like cells derived from ADSCs

ADSCs differentiated into hepatocytes over 10 days. Along with the differentiation, the cells lost fibroblastic morphology gradually and got a flatter and

broader shape. The ability of glycogen-storage of differentiated cells was analyzed using PAS staining (Fig. 4a). Results of RT-PCR and immunofluorescence revealed that liver-like cells were positive for ALB and AFP (Fig. 4b). Following 10 days of induction, the inductivity of ADSCs into hepatocytes was analyzed by flow cytometry (Fig. 4c). Results presented there were about 70.77% ADSCs successfully differentiated into hepatocytes. Furthermore, liver-like cells also secreted urea and albumin (Fig. 4d).

#### Hepatocytes transplantation decreased CCl<sub>4</sub>-induced chronic fibrosis in mouse livers

1, 2 and 3 weeks after the transplantation of hepatocytes, the liver histology was evaluated by staining with hematoxylin–eosin (H&E) (Fig. 5a), masson



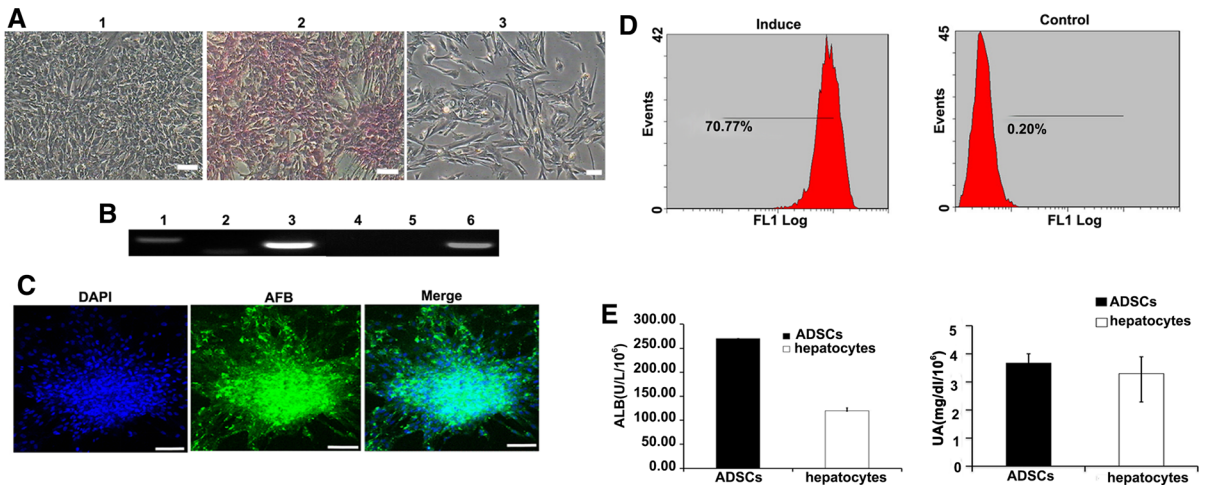


**Fig. 4** Hepatocytes induction of ADSCs. **a** Detection of morphology and glycogen staining. (1 and 2) were the induced group. 1 Pre-stain; 2 Cells were stained for glycogen. 3 Control group (bar = 100 μm). **b** RT-PCR detection of liver-specific genes such as ALB and AFP. 1, 2 and 3 for the induced group; 4, 5 and 6 for the control group; 1 and 4 were ALB, 2 and 5 were

AFP, 3 and 6 were GAPDH. **c** Immunofluorescence analysis: induced group cells were positive for specific antibody ALB. **d** Flow cytometry analyzed the inductivity of ADSCs to hepatocytes. **e** ELLSA test of ALB and UA of ADSCs and hepatocytes

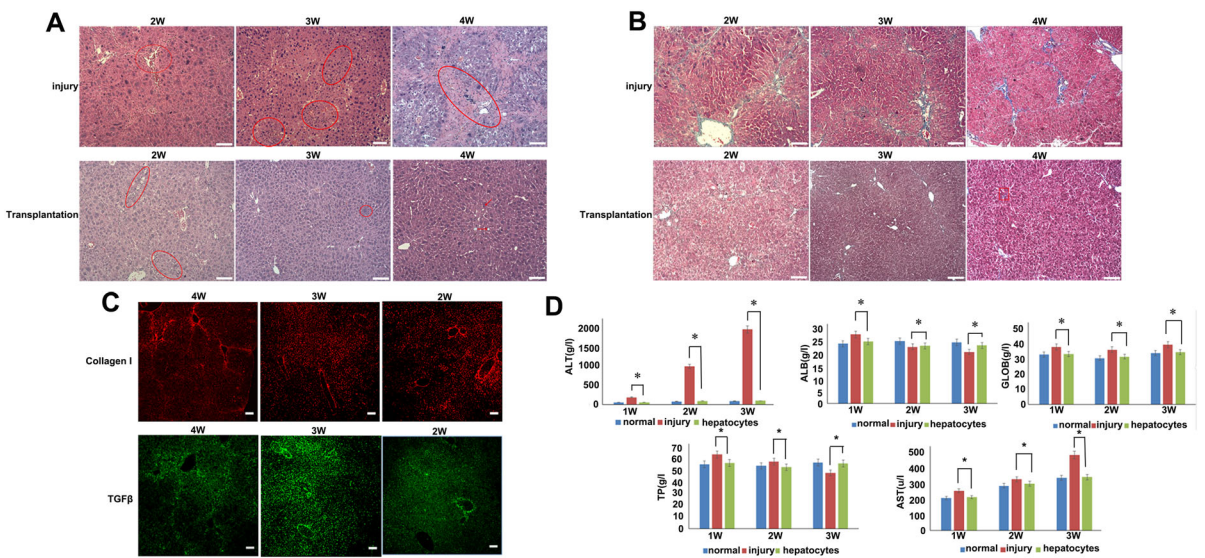


**Fig. 5 a** Hematoxylin–eosin staining of CCl<sub>4</sub>-injured liver sections after 2, 3 and 4 weeks of treatment. Control PBS (–) (upper panel) and hepatocytes transplant (lower panel). **b** Masson staining of CCl<sub>4</sub>-injured liver sections after 2, 3 and 4 weeks of treatment. Control PBS (–) (upper panel) and hepatocytes transplant (lower panel). **c** Collagen I and TGFβ

immunofluorescence staining of liver sections from mice treated for 4, 3 and 2 weeks with CCl<sub>4</sub>. **d** Biochemical markers of liver injury and function over time. ALT, ALB, GLOB, TP and AST in transplanted group returned to normal value after cell infusion, while the injury group were much higher than the normal group. \**p* < 0.05

(Fig. 5b), immunofluorescence staining for collagenase I and TGFβ expression (Fig. 5c) as well as serum transaminase levels in the three groups (Fig. 5d). All

results showed that mice presented liver injury after 4 week CCl<sub>4</sub> injection and the disease could be cured after cell transplantation.

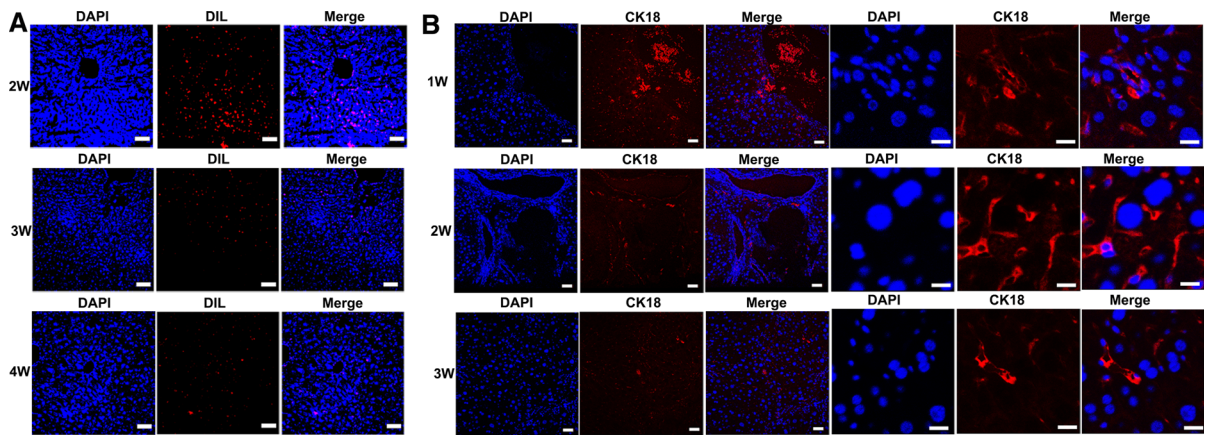


**Fig. 6** **a** Localization of hepatocytes in  $\text{CCl}_4$ -treated liver in vivo 2, 3 and 4 weeks after transplantation of cells. **b** Detection of hepatic markers in liver sections (the left part

of **b** is  $\times 100$  and the right part of **b** is  $\times 400$ , bar = 100  $\mu\text{m}$ ). Evaluation of a CK18 expression by immunofluorescence staining. Dil is a cell membrane red fluorescent dye

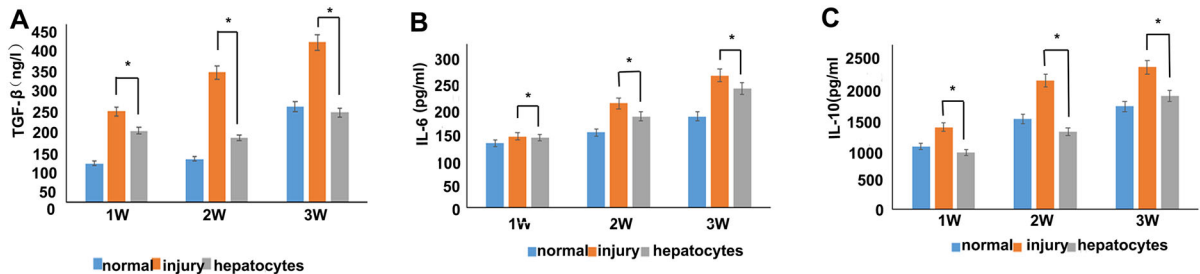


**Fig. 7** Concentration profile of interleukin 6 (IL-6), IL-10 and  $\text{TGF}\beta$  (pg/mL) in normal mice liver serum, injury mice liver serum and hepatocytes injected mice liver serum (combined the donor 1, 2 and 3). \* $p < 0.05$

#### Distribution of hepatocytes after intraportal transplantation

We detected the hepatocytes derived from ADSCs by dil-labeled frozen section (Fig. 6a) and immunofluorescence staining with CK18 for the paraffin section (Fig. 6b). CK18 served as a specific marker of hepatocytes, only reacts with the hepatocytes of Bama miniature, and does not react with the hepatocytes from mouse. After transplantation into a mouse, hepatocytes derived from ADSCs retained hepatic characteristics and functions, which showed the function of the integration of transplanted cells into the liver of mouse. Evidence of fusion between transplanted hepatocytes derived from ADSCs and mouse host hepatocytes was not found in the study.

#### Biochemical serum profile cytokines secreted by hepatocytes derived from ADSCs

To determine the cytokine profile of hepatocytes derived from ADSCs, ELISA study was conducted for cytokine concentration. As control, normal and injury group sera were analyzed, respectively. Results significantly suggested the enhanced production of  $\text{TGF}\beta$ , IL-6 and IL-10 versus normal and injury group (Fig. 7). Most reports suggest that stem cell treatment of liver failure depends mainly on the release of immunomodulatory and trophic factors (Parekkadan et al. 2007; Kharaziha et al. 2009; Xagorari et al. 2013; Jang et al. 2014).  $\text{TGF}\beta$  is an anti-fibrotic factor, interleukin (IL-6) and IL-10 are anti-inflammatory. It has been reported that IL-6 derived from intrahepatic biliary epithelial cells and had great significance in mediating the function of immune system and the regeneration of liver in vivo (Yokoyama et al. 2006;

Komori et al. 2007). Cells regulated the recovery of damaged liver function through the increasing anti-inflammatory cytokine IL-10 and therefore promote hepatocyte generation (Volarevic et al. 2010, 2011). Inhibition of autophagy could block the effects of ADSCs-derived hepatocytes on down-regulation of TGF $\beta$  expression. Our study is consistent with other reports that autophagy participated in the regulation of TGF $\beta$  synthesis.

## Discussion

Liver failure is accompanied by various pathological changes of liver disease, which can be developed into liver fibrosis, liver cirrhosis and liver cancer (Zhang et al. 2017a, b). Stem cell therapy is an effective treatment method compared with liver transplantation. Here, hepatocytes induced by ADSCs were injected via tail vein 1, 2 and 3 weeks after 4 weeks CCl<sub>4</sub> treatment mice and used to treat the acute liver failure.

In general, the functional induction of ADSCs into hepatocytes firstly evaluated. The induced cells were confirmed by morphology, glycogen staining, RT-PCR and immunofluorescence staining. Morphological observation indicated that the cells changed from fibroblasts-like to ovoid-like. AFP and ALB were the specific markers for hepatocytes. AFP is a cytoplasmic protein secreted by hepatic progenitor cells and its expression decreased with the maturation of the hepatocytes. ALB is secreted mainly by the mature hepatocytes. Detection of AFP and ALB by RT-PCR and immunofluorescence staining were used to confirm the success of induction from gene and protein level. Liver worked as the most important place of synthesis and storage of glycogen. One function of hepatocytes was glycogen synthesis. The positive result of glycogen staining suggested that the induced cells were successfully induced into hepatocytes with glycogen synthesis ability. Ammonia is a toxic substance in the body and needs to be discharged through the liver into the nontoxic urea. Detection of urea could be used to assess the metabolic function of hepatocytes. In our study, urea and ALB were detected by Elisa. All results indicated that ADSCs were successfully induced into functional hepatocytes.

ADSCs have low immunogenicity and low level of human leucocyte antigen expression. ADSCs did not express HLA-DR (MHC-II type antigen) (Tsuji et al.

2010). ADSCs are widely used in cell transplantation for their good immune tolerance and negative immunomodulation. Furthermore, ADSCs can also secrete various negative immune regulators and anti-inflammatory factors such as hepatocyte growth factors, IL-10, prostaglandin E2 etc. All these studies proved that the xenogeneic ADSCs derived from Bama miniature pig did not cause immune rejection in a mouse model and have a potential in tissue therapy.

ADSCs were mainly transplanted by the tail vein in our study. Compared with other therapies, caudal vein injection has the advantages of simple operation, small trauma, low risk and wider cell distribution. The speed of transplantation and the amount of injected cells could be controlled in our experiments. ADSCs could migrate to the liver tissue after tail vein injection and repaired the failure. In order to further explore the possibility of cell migration, we detected the dil-labeled hepatocytes by immunohistochemistry. The results showed that the transplanted cells could migrate to the liver while the number of cells decreased gradually along with the time. It is inferred that transplantation can stimulate the residual liver stem cells proliferation and decrease the positive dil-labeled cells number.

Although serological analysis confirmed that the transplanted cells could alleviate the liver injury, the mechanism was not clear. The repair of liver injury is a complex process and there are many kinds of cells and factors involved. Under what circumstances do they participate? Which stage of injury repair do they participate in? What kind of signal pathway was involved? All these questions need to be figured out in the future.

## Conclusion

Despite extensive studies on the ADSCs mediated acute liver injury repair, still little is known about the functional induced hepatocytes in the repair of acute liver failure. This study provides a basis for ADSCs derived hepatocytes in the treatment of hepatic fibrosis. According to the above investigation and discussion, some key conclusions can be drawn as follows:

- (1) ADSCs can be isolated and cultured from Bama miniature pig adipose tissue, and can be induced



as functional hepatocytes in one-step method. The induction can be identified by ELISA and flow cytometry in vitro;

- (2) Induced hepatocytes can alleviate the symptoms of acute liver failure and prove their potential for immunological rejection in heterologous cells.
- (3) The induced hepatocytes could alleviate the symptoms of acute liver failure and prove their potential for immune rejection in heterogenous cell.

**Acknowledgements** This research was funded by the National Natural Science Foundation of China (Grant No.: 31472099; 31672404), the Agricultural Science and Technology Innovation Program (ASTIP) (cxgc-ias-01) and the project National Infrastructure of Animal Germplasm Resources (2016 year).

## References

- Asrani SK, Larson JJ, Yawn B, Therneau TM, Kim WR (2013) Underestimation of liver-related mortality in the United States. *Gastroenterol* 145:375–382. <https://doi.org/10.1053/j.gastro.2013.04.005>
- Bai C, Li X, Hou L, Zhang M, Guan W, Ma Y (2013) Biological characterization of chicken mesenchymal stem/progenitor cells from umbilical cord Wharton's Jelly. *Mol Cell Biochem* 376:95–102. <https://doi.org/10.1007/s11010-012-1553-y>
- Carvalho AB, Quintanilha LF, Dias JV, Paredes BD, Manheimer EG, Carvalho FG, Asensi KD, Gutfilen B, Fonseca FM, Resende CM, Rezende GF, Takiya CM, de Carvalho AC, Goldenberg RC (2008) Bone marrow multipotent mesenchymal stromal cells do not reduce fibrosis or improve function in a rat model of severe chronic liver injury. *Stem Cells* 26:1307–1314. <https://doi.org/10.1634/stemcells.2007-0941>
- Dhawan A, Puppi J, Hughes RD, Mitry RR (2010) Human hepatocyte transplantation: current experience and future challenges. *Nat Rev Gastroenterol Hepatol* 7:7288–7298. <https://doi.org/10.1038/nrgastro.2010.44>
- Jang YO, Kim YJ, Baik SK, Kim MY, Eom YW, Cho MY, Park HJ, Park SY, Kim BR, Kim JW, Soo Kim H, Kwon SO, Choi EH, Kim YM (2014) Histological improvement following administration of autologous bone marrow-derived mesenchymal stem cells for alcoholic cirrhosis: a pilot study. *Liver Int* 34:33–41. <https://doi.org/10.1111/liv.12218>
- Kharaziha P, Hellstrom PM, Noorinayer B, Farzaneh F, Aghajani K, Jafari F, Telkabadi M, Atashi A, Honardoost M, Zali MR, Soleimani M (2009) Improvement of liver function in liver cirrhosis patients after autologous mesenchymal stem cell injection: a phase I-II clinical trial. *Eur J Gastroenterol Hepatol* 21:1199–1205. <https://doi.org/10.1097/MEG.0b013e32832a1f6c>
- Khurana S, Mukhopadhyay A (2007) Characterization of the potential subpopulation of bone marrow cells involved in the repair of injured liver tissue. *Stem Cells* 25:1439–1447. <https://doi.org/10.1634/stemcells.2006-0656>
- Komori A, Nakamura M, Fujiwara S, Yano K, Fujioka H, Migita K, Yatsuhashi H, Ishibashi H (2007) Human intrahepatic biliary epithelial cell as a possible modulator of hepatic regeneration: Potential role of biliary epithelial cell for hepatic remodeling in vivo. *Hepatol Res* 37:443. <https://doi.org/10.1111/j.1872-034X.2007.00237.x>
- Lee KD, Kuo TK, Whang-Peng J, Chung YF, Lin CT, Chou SH, Chen JR, Chen YP, Lee OK (2004) In vitro hepatic differentiation of human mesenchymal stem cells. *Hepatology* 40:1275–1284. <https://doi.org/10.1002/hep.20469>
- Ma C, Liu C, Li X, Lu T, Bai C, Fan Y, Guan W, Guo Y (2017) Cryopreservation and multipotential characteristics evaluation of a novel type of mesenchymal stem cells derived from Small Tailed Han Sheep fetal lung tissue. *Cryobiology* 75:7–14. <https://doi.org/10.1016/j.cryobiol.2017.03.003>
- Mendizabal M, Silva MO (2016) Liver transplantation in acute liver failure: a challenging scenario. *World J Gastroenterol* 22:1523. <https://doi.org/10.3748/wjg.v22.i4.1523>
- Ong SH, Dai H, Leong KW (2006a) Inducing hepatic differentiation of human mesenchymal stem cells in pellet culture. *Biomaterials* 27:4087–4097. <https://doi.org/10.1016/j.biomaterials.2006.03.022>
- Ong SY, Dai H, Leong KW (2006b) Hepatic differentiation potential of commercially available human mesenchymal stem cells. *Tissue Eng* 12:3477–3485. <https://doi.org/10.1089/ten.2006.12.3477>
- Parekkadan B, van Poll D, Sukanuma K, Carter EA, Berthiaume F, Tilles AW, Yarmush ML (2007) Mesenchymal stem cell-derived molecules reverse fulminant hepatic failure. *PLoS ONE* 2:e941. <https://doi.org/10.1371/journal.pone.0000941>
- Schuessler K, Pignitter M, Somoza V (2015) Sulfated and glucuronated trans-resveratrol metabolites regulate chemokines and sirtuin-1 expression in U-937 macrophages. *J Agric Food Chem* 63:6535–6545. <https://doi.org/10.1021/acs.jafc.5b01830>
- Schuessler F, Roy S, Loosen SH, Alder J, Koppe C, Schneider AT, Wandrer F, Bantel H, Vucur M, Mi QS, Trautwein C, Luedde T, Roderburg C (2017) miR-223 represents a biomarker in acute and chronic liver injury. *Clin Sci* 131:1971–1987. <https://doi.org/10.1042/CS20170218>
- Terai T, Ishikawa T, Omori K, Aoyama K, Marumoto Y, Urata Y, Yokoyama Y, Uchida K, Yamasaki T, Fujii Y, Okita K, Sakaïda I (2006) Improved liver function in patients with liver cirrhosis after autologous bone marrow cell infusion therapy. *Stem Cells* 24:2292–2298. <https://doi.org/10.1634/stemcells.2005-0542>
- Terry C, Hughes RD, Mitry RR, Lehec SC, Dhawan A (2007) Cryopreservation-induced nonattachment of human hepatocytes: role of adhesion molecules. *Cell Transplant* 16:639–647. <https://doi.org/10.3727/000000007783465000>
- Tsuji H, Miyoshi S, Ikegami Y, Hida N, Asada H, Togashi I, Suzuki J, Satake M, Nakamizo H, Tanaka M, Mori T, Segawa K, Nishiyama N, Inoue J, Makino H, Miyado K, Ogawa S, Yoshimura Y, A Umezawa (2010) Xenografted



- human amniotic membrane-derived mesenchymal stem cells are immunologically tolerated and transdifferentiated into cardiomyocytes. *Circ Res* 106:1613–1623. <https://doi.org/10.1161/CIRCRESAHA.109.205260>
- Volarevic V, Al-Qahtani A, Arsenijevic N, Pajovic S, Lukic ML (2010) Interleukin-1 receptor antagonist (IL-1Ra) and IL-1Ra producing mesenchymal stem cells as modulators of diabetogenesis. *Autoimmunity* 43:255–263. <https://doi.org/10.3109/08916930903305641>
- Volarevic V, Arsenijevic N, Lukic ML, Stojkovic M (2011) Concise review: mesenchymal stem cell treatment of the complications of diabetes mellitus. *Stem Cells* 29:5–10. <https://doi.org/10.1002/stem.556>
- Wei JF, Li HL, Wang SH, Li TP, Fan JF, Liang XL, Li J, Han Q, Zhu L, Fan LY, Zhao RC (2014) Let-7 enhances osteogenesis and bone formation while repressing adipogenesis of human stromal/mesenchymal stem cells by regulating HMGA2. *Stem Cells Dev* 23:1452–1463. <https://doi.org/10.1089/scd.2013.0600>
- Xagorari A, Siotou E, Yiangou M, Tsolaki E, Bougiouklis D, Sakkas L, Fassas A, Anagnostopoulos A (2013) Protective effect of mesenchymal stem cell-conditioned medium on hepatic cell apoptosis after acute liver injury. *Int J Clin Exp Pathol* 6:831–840. ISSN 1936-2625/IJCEP1302004
- Yokoyama T, Komori A, Nakamura M, Takii Y, Kamihira T, Shimoda S, Mori T, Fujiwara S, Koyabu M, Taniguchi K, Fujioka H, Migita K, Yatsunami H, Ishibashi H (2006) Human intrahepatic biliary epithelial cells function in innate immunity by producing IL-6 and IL-8 via the TLR4/NF-kappaB and -MAPK signaling pathways. *Liver Int* 26:467–476. <https://doi.org/10.1111/j.14783231.2006.01254.x>
- Zaret KS, Grompe M (2008) Generation and regeneration of cells of the liver and pancreas. *Science* 322:1490–1494. <https://doi.org/10.1126/science.1161431>
- Zhan Y, Wang Y, Wei L, Chen H, Cong X, Fei R, Gao Y, Liu F (2006) Differentiation of hematopoietic stem cells into hepatocytes in liver fibrosis in rats. *Transpl Proc* 38:3082–3085. <https://doi.org/10.1016/j.transproceed.2006.08.132>
- Zhang S, Bai CY, Zheng D, Gao YH, Fan YN, Li L, Guan WJ, Ma YH (2017a) Identification and characterization of pig adipose-derived progenitor cells. *Can J Vet Res* 80:309–317
- Zhang X, Ding J, Gou C, Wen T, Li L, Wang X, Yang H, Liu D, Lou J, Chen D, Ren F, Li X (2017b) Qingchangligan formula attenuates the inflammatory response to protect the liver from acute failure induced by d-galactosamine/lipopolysaccharide in mice. *J Ethnopharmacol* 201:108–116. <https://doi.org/10.1016/j.jep.2016.11.007>